

In vivo imaging of subcutaneous structures using functional photoacoustic microscopy

Hao F Zhang¹, Konstantin Maslov¹ & Lihong V Wang

Department of Biomedical Engineering, Washington University in St. Louis, St. Louis, Missouri 63130, USA. ¹These authors contributed equally to this work. Correspondence should be addressed to L.V.W. (lhwang@biomed.wustl.edu).

Published online 5 April 2007; doi:10.1038/nprot.2007.108

Functional photoacoustic microscopy (fPAM) is a hybrid technology that permits noninvasive imaging of the optical absorption contrast in subcutaneous biological tissues. fPAM uses a focused ultrasonic transducer to detect high-frequency photoacoustic (PA) signals. Volumetric images of biological tissues can be formed by two-dimensional raster scanning, and functional parameters can be further extracted from spectral measurements. fPAM is safe and applicable to animals as well as humans. This protocol provides guidelines for parameter selection, system alignment, imaging operation, laser safety and data processing for *in vivo* fPAM. It currently takes ~100 min to carry out this protocol, including ~50 min for data acquisition using a 10-Hz pulse-repetition-rate laser system. The data acquisition time, however, can be significantly reduced by using a laser system with a higher pulse repetition rate.

INTRODUCTION

PA imaging is a hybrid technology that images the internal distribution of optical energy deposition in biological tissues based on the detection of laser-induced ultrasonic waves (referred to as PA or optoacoustic waves)^{1–8}, which reveals physiologically specific optical absorption contrast. It provides high spatial resolution in deep biological tissues compared to traditional optical imaging^{9,10} by taking advantage of the weaker ultrasonic scattering, whose magnitude is two orders of magnitude less than that of optical scattering¹¹. Moreover, by varying the optical wavelength of the excitation laser to conduct spectral measurement, PA imaging is able to extract certain functional parameters, such as the hemoglobin oxygenation saturation (sO₂), without using exogenous contrast agents.

Two major forms of PA imaging have been actively studied: photoacoustic tomography (PAT)^{2,3,5} and photoacoustic microscopy (PAM)⁴. Typical PAT uses an unfocused ultrasound detector/array and an inverse algorithm to reconstruct cross-sectional or three-dimensional images of biological samples. The geometry of optical energy delivery and acoustic detection in PAT can be in orthogonal, reflection (backward) or transmission (forward) mode. Readers are referred to reviews and research articles for more details^{1–3,5}. Compared with PAT, PAM uses a spherically focused ultrasonic detector and requires no reconstruction algorithm. Moreover, PAM typically works in a reflection mode and uses higher ultrasonic frequencies than PAT to achieve better spatial resolution. Although various methods for light delivery can be applied, an optical-ultrasonic confocal illumination improves the signal-to-noise ratio (SNR).

We recently developed the fPAM^{12,13} that achieved much improved image quality at greater depth by using dark-field illumination with a large illumination area in contrast to the previously published PAM⁴. fPAM provides an axial resolution of 15 μm and a lateral resolution of 45 μm with a maximum imaging depth of 3 mm. Based on intrinsic optical absorbing pigments, such as hemoglobin and melanin, in biological tissues, fPAM has been applied to image the morphology of the subcutaneous microvasculature¹⁴, sO₂ in the microvasculature^{13,15}, skin melanoma tumors¹⁶ and acute skin burns¹⁷. If bioconjugated contrast agents

are administered, fPAM can also be applied to image molecular and genetic contrasts such as imaging of LacZ genetic expression¹⁸. fPAM is safe and can be applied to human imaging. However, in this protocol, we take rats and mice as examples.

Equipment setup

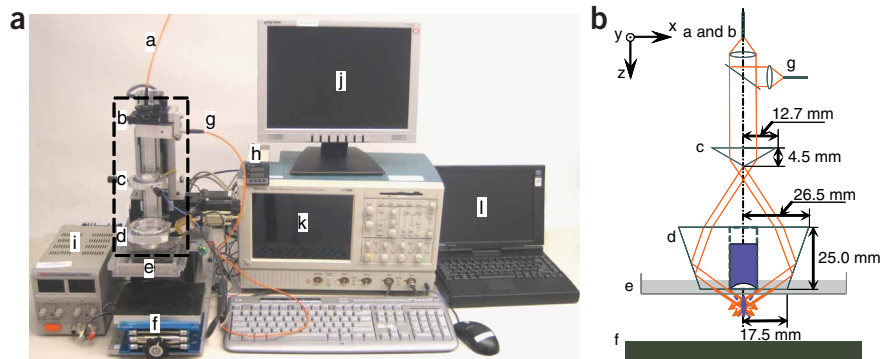
The fPAM (**Fig. 1**) consists of three major subsystems: a tunable pulsed laser system, an imaging head mounted on computer-controlled mechanical scanner and a data acquisition system. For the coordination of the subsystems, a synchronization signal is required, which can be generated from the laser system, the motor-controlling system or the data acquisition system. Currently, the synchronization signal is provided by the laser system. The data acquisition system receives synchronization pulses from the laser system and relays them to the motor-controlling system.

The laser system needs to produce laser pulses short enough (several nanoseconds) in order to generate short PA pulses that provide high spatial resolution⁴. The current fPAM uses a tunable dye laser that is pumped by a Q-switched Nd:YAG laser as the irradiation source, which has a pulse duration of 6.5 ns and a pulse repetition rate of 10 Hz. However, other types of tunable laser system are also available. In fact, a laser system with high pulse repetition rate is desired for fast image acquisition. The laser system should also be able to supply sufficient output energy to ensure good SNR. The current fPAM requires 0.2 mJ per pulse to be delivered to biological samples (see Laser safety).

The imaging head (**Fig. 1b**) consists of four major components: a multi-axis fiber positioner with a focusing lens, a conical lens, an optical condenser and a focused ultrasonic transducer. The conical lens and the optical condenser are custom-made components, whose physical dimensions are given in **Figure 1b**. The focused ultrasonic transducer is modified from a commercial broadband delay-line transducer (V214-BB-RM, Panametrics) by grinding a concave spherical cavity directly in its quartz delay line (**Fig. 1b**). This concave cavity works as a focusing acoustic lens. For raster scanning, the imaging head is mounted on a motorized translation stage, which is directed by the motor-controlling PC.

PROTOCOL

Figure 1 | Instrument of fPAM. (a) Photograph of fPAM. The tunable laser system is not shown and the imaging head is highlighted by the dashed-box. (a) Source fiber. (b) Multi-axis fiber positioner with a focusing lens. (c) Conical lens. (d) Optical condenser and focused ultrasonic detector. (e) Water container with a window at its bottom sealed with an optically and ultrasonically transparent disposable polyethylene membrane. (f) Animal holder. (g) Beam sampler and reference fiber. (h) Temperature controller. (i) Motor power supply. (j) Commanding monitor for data acquisition PC, which is integrated with the digital oscilloscope. (k) Digital oscilloscope. (l) Motor-controlling PC. (b) Schematic of the imaging head. The conical lens is made from BK7 glass and the optical condenser is made from acrylic. The diameter of the concave spherical cavity in the quartz delay line of the commercial ultrasonic detector and its radius of curvature are 5.8 and 4.8 mm, respectively. The focal length of this modified transducer is 6.7 mm and the focal diameter (-6 dB) is $45\ \mu\text{m}$ in its focal zone in water.



The motor-controlling program has two execution modes: command mode (C mode) and free-running mode (F mode). In C mode, no synchronization signal is required. Users can adjust the height and the horizontal position of the imaging head to match the region of interest (ROI). In F mode, users need to specify, before scanning, the motor-controlling parameters (scanning ranges and scanning step sizes), the number of optical wavelengths and the value of each wavelength. Once the F-mode scanning starts, the motor-controlling PC directs the raster scanning and sends commands to the laser system to change the optical wavelength automatically.

The current fPAM uses a wideband preamplifier (0.1–500 MHz) to amplify the detected PA signals by 24 dB. A digital oscilloscope is employed as both the signal digitizer and the data acquisition PC. The digital oscilloscope is based on the MS Windows 2000 operational system. The data acquisition program written in Matlab can communicate with the oscilloscope through a virtual GPIB card faster than through a conventional GPIB card (for more

details, refer to <http://www.ni.com/gpib/>). A digital acquisition board may also be used as a signal digitizer provided that its sampling rate, bandwidth and dynamic range meet the requirements. The current oscilloscope has a maximum single-channel sampling rate of 5 GHz, a bandwidth of 350 MHz and a dynamic range of 48 dB (8-bit digitizer resolution). A fast photodiode is used to detect the laser pulse energy as a reference to compensate for the instability of the laser output. Before starting the F-mode automatic scanning, users must also input the motor-controlling parameters and the number of wavelengths to the data acquisition program accordingly. Users need to specify further the holding time in the data acquisition program so that enough time is allocated between B scans (see image acquisition) for the translation stage to return to its initial x position and for the laser system to change the output optical wavelength. In addition, users need to adjust the electrical parameters before acquiring images (for details about the motor-controlling and the electrical parameters, please see Know your sample and choose correct parameters section).

During the F-mode scanning, the data acquisition PC stores the digitized PA signals transferred from the oscilloscope. When one B scan is completed, the data acquisition PC blocks the synchronization pulses from the motor-controlling system during the holding time.

Image acquisition

The fPAM acquires an image by recording time-resolved PA signals at each point in a 2D raster scan along a horizontal (x - y) plane (Fig. 2). For each laser pulse, fPAM acquires a time-resolved PA signal and a reference signal of the pulse energy. Then fPAM translates the imaging head by one scanning step along the x axis and awaits the next laser pulse. Once the lateral scan along the x axis (B scan) is completed, the imaging head is returned to its initial x coordinate, and is further translated by one scanning step along the y axis to start a new B scan. Meanwhile, the PA and the reference signals

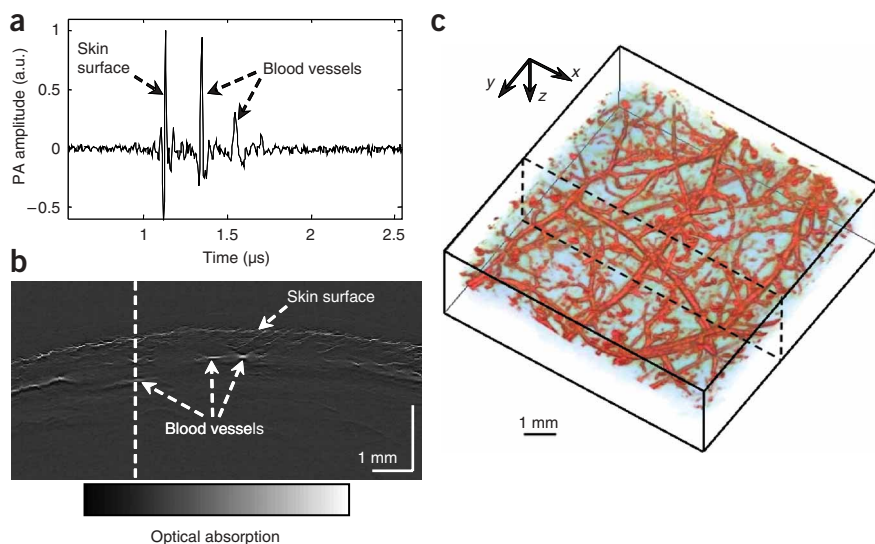


Figure 2 | Image acquisition by fPAM. (a) A line at the location marked with a dashed line in c. In this specific case, the peak amplitudes of PA signals that correspond to the skin surface and the shallow subcutaneous blood vessels are comparable. (b) B-scan image at the location marked with a dashed box in c. (c) Pseudocolor volumetric visualization of the microvasculature with skin signals removed.

that are digitized and stored in the channel memory of the oscilloscope in the previous B scan are transferred to the data acquisition PC and saved to the hard disk. In spectroscopic imaging, the optical wavelength is changed after each B scan is completed. When the entire 2D scan is finished, the imaging head is translated back to its initial coordinates.

An A line (Fig. 2a) is a one-dimensional depth-resolved (along the z axis) image converted from the time-resolved PA signal based on the sound velocity in tissue ($1.54 \text{ mm } \mu\text{s}^{-1}$). A B-scan image (Fig. 2b) is formed by assembling A lines with identical y coordinate into a 2D cross-sectional (along the z - x plane) image. With all the B-scan images combined, the final volumetric data can be visualized three-dimensionally (Fig. 2c).

Know your sample and choose correct parameters

Optical wavelengths As fPAM images the optical absorption contrast, users need to analyze the optical extinction spectra of the target endogenous pigments or exogenous contrast agents to choose the optimal optical wavelengths for various imaging purposes.

- Structural imaging of blood vessels. Users should choose optical wavelengths according to the molar extinction coefficient spectra of both oxyhemoglobin (HbO_2) and deoxyhemoglobin (HbR) (for lists of values, refer to <http://omlc.ogi.edu/spectra/>) (Fig. 3). For the purpose of imaging veins and arteries equally well, the suitable optical wavelengths should be those at which HbO_2 and HbR have identical molar extinction coefficients (isosbestic points). At these wavelengths, the image contrast reflects the total hemoglobin concentration. To achieve high image contrast, the optical absorption of blood needs to be strong at those wavelengths compared with that of the surrounding tissues. As a result, the optimal optical wavelengths are, for example, 529, 545, 570 and 584 nm.
- Functional imaging of blood vessels. To extract functional parameters such as $s\text{O}_2$, spectral measurement is required. First of all, users need to choose wavelengths with strong optical absorption of hemoglobin to ensure good SNR. Moreover, users should choose a proper spectral range within which the inversion error is minimized¹⁹. A practical limitation in selecting a proper spectral range in our experiments comes from the fact that typical commercial dye lasers have a continuous optical wavelength tuning range of less than 30 nm using a single dye solution. In principle, two optical wavelengths are enough to

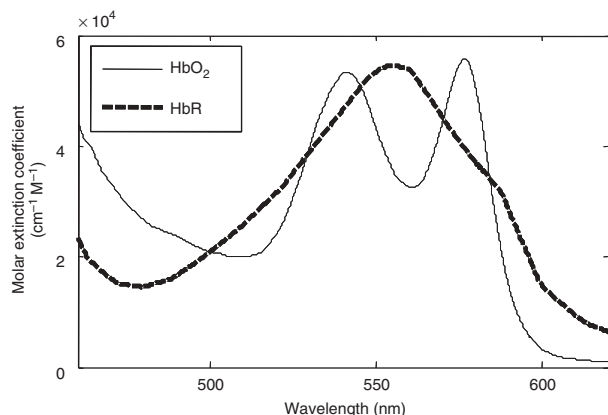


Figure 3 | Molar extinction coefficient spectra of human hemoglobin.

determine $s\text{O}_2$ in the simplest model. Users should employ more optical wavelengths for better accuracy. However, increasing the number of optical wavelengths prolongs the data acquisition time. Based on our estimation, good spectral ranges are between 550 and 600 nm and between 700 and 760 nm when using four equally spaced optical wavelengths with a spacing of a few nanometers¹⁹. However, if a different number of optical wavelengths, nonuniform wavelength spacing or a laser system with a wider continuous optical wavelength tuning range (such as an optical parametric oscillator system) is used, the above analysis would be modified accordingly.

- Imaging of other endogenous pigments or exogenous contrast agents. As blood is the dominating optical absorber, the general rule for this imaging purpose is to find optical wavelengths so that the contrast between the target optical absorption and the blood absorption is maximized. However, if the optical absorption of the target pigment or contrast agent is weaker than that of hemoglobin within a wide spectral range, users need to consider multiwavelength imaging rather than single-wavelength imaging. In choosing optical wavelengths for multiwavelength imaging, the rules stated above for functional imaging of blood vessels also apply. Moreover, in the inverse calculation of the concentration distributions of the target absorbers, the presence of HbO_2 and HbR must also be taken into consideration. Hence, at least three concentrations must be estimated, which implies that at least three optical wavelengths have to be used.

Ultrasonic parameters The lateral resolution of fPAM in biological tissues is mainly determined by the center frequency and the numerical aperture (NA) of the ultrasonic detector, and the axial resolution is primarily determined by the frequency bandwidth of the ultrasonic detector²⁰. Therefore, users need to choose the ultrasonic parameters according to the structures to be resolved. For example, if the target blood vessel has a diameter of around 100 μm , an ultrasonic transducer with a center frequency of 50 MHz, a bandwidth of 70% and an NA of 0.44, which gives a lateral resolution of 45 μm and an axial resolution of 15 μm , is suitable¹³. The center frequency, however, is also limited by the target imaging depth owing to the frequency-dependent acoustic attenuation. Using an ultrasonic transducer with the above parameters, the maximum imaging depth in biological tissues is 3 mm. If deeper imaging is required, the center frequency needs to be reduced accordingly, which degrades the spatial resolution. Therefore, a trade-off is necessary between the maximum imaging depth and the spatial resolution.

Motor-controlling parameters The motor-controlling parameters include the scanning ranges and the scanning step sizes along both the x and y axes. The scanning ranges are determined by the size of the ROI, and the scanning step sizes should equal the estimated lateral resolution in general. Using finer step sizes improves the image quality but prolongs the data acquisition. The step sizes along the two axes can be different but are identical in the current fPAM.

Electrical parameters The electrical parameters include the sampling rate, trigger delay and recording length. The sampling

rate should satisfy the Nyquist sampling theory based on the cutoff frequency of the ultrasonic detector. A practical value is 4–5 times of the center ultrasonic frequency. After mechanically aligning the ultrasonic focus with the expected center depth (along the *z* axis) of the field of view (FOV), the trigger delay is adjusted according to the ultrasonic focal length and the distance between the ultrasonic detector and the sample surface so that PA signals from the FOV can be recorded. The recording length is determined by the desired FOV along the *z* axis. For example, an FOV of 3 mm in biological tissues requires a 2- μ s recording length.

System alignment

As fPAM is a confocal imaging system, good alignment of the optical-ultrasonic dual foci is essential for high-quality imaging. The following procedure should be followed:

- Adjust the distance between the conical lens and the optical condenser (Fig. 1b) to overlap the optical focus with the ultrasonic focus along the vertical axis. Users can place an optical absorbing object with a flat surface around the ultrasonic focus and observe the amplitude of the PA peak generated from the surface. Adjust the distance until the PA peak reaches its maximum amplitude.
- Adjust the horizontal positions of the fiber positioner and the conical lens to overlap the optical focus with the ultrasonic focus in the horizontal plane. Users can acquire B-scan images of a cross-section of a spherical or a cylindrical object (with a diameter less than half of the lateral resolution of fPAM) along both the *x* and *y* axes to visualize the adjustment. A sample B-scan image of a carbon fiber with good alignment is shown in Figure 4, where symmetries along both the vertical and the lateral directions are observed.
- Repeat the above steps if necessary.

Laser safety

Users can achieve high SNR and fast imaging acquisition by using strong laser pulses and high pulse repetition rate, respectively. When fPAM is used to image human subjects *in vivo*, however, the maximum permissible pulse energy and the maximum permissible pulse repetition rate are governed by the ANSI laser safety

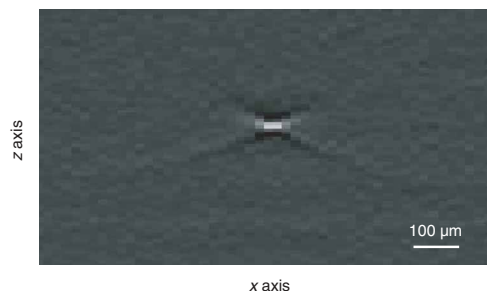


Figure 4 | B-scan image of the cross-section of a carbon fiber (diameter: 6 μ m) immersed in an optically scattering medium. The optical-ultrasonic dual foci are well aligned and the carbon fiber is placed around the ultrasonic focal point.

standards²¹. The safety limits for the skin depend on the optical wavelength, pulse duration, exposure duration and exposure aperture. For the current fPAM, the following standards apply. In the visible spectrum (400–700 nm), the exposure on the skin surface by any single laser pulse should not exceed 20 mJ cm⁻²; the current fPAM has less than 6.4 mJ cm⁻² (pulse energy: 0.2 mJ; diameter of the illumination area at the ultrasonic focus in an optically clear medium: 2 mm). In addition, if a point on the skin is exposed to laser light for more than 10 s, the mean irradiance should not exceed 200 mW cm⁻², which results in a maximum permissible repetition rate of 30 Hz here. In raster scanning, the exposure duration of a point on the skin surface is typically less than 10 s. In this case, the maximum permissible exposure is limited by $1,100t_e^{1/4}$ in mJ cm⁻², where t_e denotes the exposure duration in seconds. This limit translates into $E \times \sqrt{F} \leq 2.75 \times 10^2 \pi d^{5/4} (\Delta/N)^{3/4}$, where E denotes the pulse energy in mJ, F denotes the pulse repetition rate in Hz, d denotes the diameter of the illumination area at the ultrasonic focus in cm, Δ denotes the scanning step size in cm and N denotes the number of laser pulses at each scanning step (for signal averaging, for example). Based on the parameters of the current fPAM ($N = 1$), F can be up to 13 kHz. In other specific scanning schemes, users should verify the conformance to the safety standards separately.

MATERIALS

REAGENTS

- Sprague–Dawley rats (Charles River Breeding Laboratories, 150–200 g)
- Immunocompromised nude mice (Harlan, 20 g) **▲ CRITICAL** Users can apply fPAM to image various anatomical sites of animals or humans. Here, we take rats and mice as examples. **! CAUTION** All experimental animal and human procedures should be carried out in conformity with the applicable national guidelines and regulations.
- Deionized water
- Human hair-removing lotion (Surgi Cream; Ardell Int'l)
- Ultrasound gel (Clear Image; Sonotech)
- Intralipid (Liposyn II; Hospira)
- Ketamine (Ketaset; Fort Dodge Animal Health)
- Xylazine (Tranquived; VedCo)
- Isoflurane (IsoFlo; Abbott Laboratories)

EQUIPMENT

- Pulsed pump laser (Brilliant B; BigSky)
- Tunable dye laser (ND6000; Continuum) **! CAUTION** Class IV laser. Wear laser protection goggles during operation.
- Optical diffuser (DG2X2-600; Thorlabs) to attenuate and homogenize the output laser light from the tunable dye laser before light is coupled into the optical fiber, which delivers light to the imaging head

- Optical fiber (source fiber) with large (at least 600 μ m) core diameter that delivers light from the tunable dye laser to the imaging head
- Multi-axis lens positioner (LP-05A; Newport)
- Focusing lens (NT95-113; Edmund Optics)
- Beam sampler (BSP05-A1; Thorlabs)
- Conical lens made of BK7 glass (LA1951; Thorlabs) **▲ CRITICAL** The physical dimensions are given in Figure 1b.
- Optical fiber (reference fiber) with 200 μ m core diameter
- Fast photodiode (FDS010; Thorlabs)
- Optical condenser made of acrylic (8581K82; McMaster-Carr), which operates by total internal reflection **▲ CRITICAL** The physical dimensions are given in Figure 1b.
- Translation stages (KR2602A; THK)
- Step motor (NEMA 17; Anaheim Automation)
- Motor driver (MBC15161; Anaheim Automation)
- Ultrasonic transducers (V214-BB-RM, Panametrics; Alpha IPS/25.0/.25, Gamma IPS/10.0/.25, Krautkramer) **▲ CRITICAL** Users should choose an ultrasonic detector with a large numerical aperture to achieve high image quality.
- Wideband signal amplifier (ZFL-500LN; Mini-Circuits)
- Power supply (HY3005; RSR Electronics)

- Oscilloscope (TDS 5034B; Tektronix)
- Temperature controller (DC1010; Honeywell)
- Computers
- Breathing anesthesia system (E-Z Anesthesia; Euthanex)
- Pulse oximeter (8600V; Nonin Medical)
- Hair trimmer (ConairPro)
- Polyethylene membrane (Glad)
- Paper tape (3M)
- Tygon laboratory tubing (Saint-Gobain Performance Plastics)
- Commercial 3D visualization software (VolView; Kitware)
- Scientific software (Matlab; Mathworks) for developing the data acquisition program

PROCEDURE

! CAUTION For illustration, the imaging of the subcutaneous microvasculature in the dorsal area of a mouse or a rat (body weight: 20–200 g) with low skin melanin concentration is elaborated. For other imaging applications, the procedure needs to be revised accordingly.

- 1| Seal the window at the bottom of the water container with new polyethylene membrane.
- 2| Fill the water container with deionized water, which acts as an ultrasonic coupling medium between the ultrasonic detector and the sample. During raster scanning, the bottoms of the ultrasonic detector and the optical condenser are immersed in water.
- 3| Set the temperature controller to a desired temperature and turn on the heater. During the experiment, the temperature of the water and the water container is regulated around 38 °C so that the body temperature of the animal can be maintained.
- 4| Administer a dose of 87 mg kg⁻¹ ketamine plus 13 mg kg⁻¹ xylazine intramuscularly to anesthetize the animal. Wait for 10–15 min until the animal is fully anesthetized.
- 5| Trim hair in the ROI as well as the surrounding area.
- 6| Apply Surgi Cream to the trimmed area and wait for 1–4 min before cleaning with warm water.
- 7| Apply a layer of ultrasound gel (~2 mm thick) onto the depilated area.
- 8| Apply a layer of ultrasound gel at the bottom of the membrane that seals the window of the water container.
! CAUTION Avoid trapping air bubbles inside the ultrasound gel.
- 9| Place the animal on the animal holder and loosely fix the tail and two hind legs with paper tape to limit animal motion during data acquisition.
- 10| Place the ROI under the window and lift the animal holder until the animal touches the bottom of the water container.
! CAUTION Leave enough space for the animal to breathe normally.
- 11| Squeeze out some ultrasound gel so that the distance between the membrane and the skin surface is minimized. Readjust the height of the animal holder if necessary.
- 12| Supply a mixture of medical grade oxygen with 1% (volume to volume ratio) vaporized isoflurane at a flow rate of 1.5 liter per min to the animal through a nose cone.
! CAUTION Flow rate varies with the body weight of the animal. Please refer to the instructions on the specific breathing anesthesia system.
- 13| Clamp the pulse oximeter to, for example, the hind leg of the animal.
- 14| Apply neutral ointment to the animal eyes to prevent dryness and cover them to prevent accidental laser damage.
- 15| Start the motor-controlling program in C mode. Set the scanning range along the x axis and the scanning step size to the designated values, but set the scanning range along the y axis to one step size, which results in an acquisition of only one B-scan image after each F-mode scanning. For multiwavelength imaging, use a single optical wavelength at an isosbestic point temporarily.
- 16| Lower down the imaging head until the bottom of the ultrasonic detector is immersed in water using the motor-controlling program in C mode.
- 17| Remove air bubbles trapped by the concave focusing lens of the ultrasonic detector. Users can use a U-shaped plastic tube connected to a syringe to suck out the bubbles.
▲ CRITICAL STEP Trapped air bubbles should be removed completely.

PROTOCOL

18| Connect the signal amplifier and the photodiode to the oscilloscope. Input correct electrical parameters. Make sure that the dynamic range of the oscilloscope is fully used by adjusting the input-signal ranges of all channels. Adjust the channel filtering according to the center frequency and the bandwidth of the ultrasonic detector.

19| Start the laser firing.

! CAUTION The laser pulse energy and the pulse repetition rate should be verified carefully according to the laser safety.

20| Adjust the z position of the imaging head until PA signal is detected and the desired FOV along the z axis is reached. Readjust the trigger delay value and the input-signal ranges if necessary.

? TROUBLESHOOTING

21| Start the data acquisition program and input the motor-controlling parameters to the data acquisition program (keep the scanning range along the y axis equal to one scanning step size). For multiwavelength imaging, set the number of optical wavelengths to one temporarily.

22| Execute the data acquisition program and acquire one B-scan image using F-mode scanning. Check the ultrasonic focusing on the target vessels from the acquired B-scan image.

? TROUBLESHOOTING

23| Readjust the z position of the imaging head and repeat the previous step until the best ultrasonic focusing is reached. Readjust the trigger delay if necessary.

24| Change the scanning range along the y axis to the designated value in both the motor-controlling and the data acquisition programs. For multiwavelength imaging, input the correct number of optical wavelengths and their values to both the motor-controlling and the data acquisition programs.

25| Start acquiring data in F mode.

? TROUBLESHOOTING

26| Stop the laser firing once data acquisition is completed.

27| Lift the imaging head out of the water.

28| Lower down the animal holder, stop the breathing anesthesia system, release the animal and clean the ultrasound gel off the animal body.

29| If future experiments on the same animal are necessary, house the animal according to the approved animal protocols. Otherwise, euthanize and dispose of the animal by following proper procedures.

● TIMING

System and animal preparation (Steps 1–14): ~ 30 min

Adjust the z location of the imaging head for best ultrasonic focusing (Steps 15–23): ~ 10 min

Data acquisition (Steps 24–26): varies with the laser pulse repetition rate, scanning area and scanning step size. For example, single-wavelength scanning of an 8 mm by 8 mm area with a step size of 50 μm and a pulse repetition rate of 10 Hz requires ~ 50 min. In fact, we have developed a high-speed fPAM system using a laser system whose pulse repetition rate can be up to 1 kHz. This new system has a B-scan (containing 200 A-lines) frame rate of more than 1 Hz, which, however, requires modifications of the mechanical scanner and the motor-controlling system.

Remaining procedures (Steps 27–29): ~ 10 min

Total time: ~ 100 min

? TROUBLESHOOTING

No PA signal (Step 20)

First, make sure that the signal amplifier is powered and all cables are functioning properly and are connected correctly. Second, make sure that air bubbles trapped by the ultrasonic detector are completely removed. Third, make sure that enough laser light is delivered to the sample.

To locate PA signals initially, users can set the trigger delay to zero and set the recording length to a few times longer than the recording length required for the expected FOV along the z axis. Then, adjust the z position of the imaging head until a PA signal (with at least one peak corresponding to the skin surface) is observed in the oscilloscope. The PA peaks should shift in time when the z position of the imaging head changes. Finally, adjust the trigger delay and recording length to match the desired FOV along the z axis.

PA signals generated from the skin surface are too strong (Step 22)

If the skin is cleaned and depilated, this problem is most probably caused by poor system alignment, which means that the optical focus is above the ultrasonic focus along the z axis. Users can temporarily ease this problem by adjusting the distance between the conical lens and the ultrasound detector. However, a realignment of the confocal system is preferred.

Strong motion artifact (Step 25)

The major motion artifact comes from the breathing motion of the animals. Make sure that the nose cone is properly placed and the breathing anesthesia system is functioning properly. Check the animal holding and make sure that the animals can breathe freely. A water container with a bottom window size comparable with the size of the ROI can help minimize the motion artifact.

Incorrect optical wavelength changing (Step 25)

In the current multiwavelength fPAM imaging, the optical wavelength is changed after each B-scan image (rather than A line) is acquired to minimize the total data acquisition time. Depending on the range of the desired optical wavelength change, mechanical wavelength tuning can take several seconds. In this case, users need to leave enough holding time between B scans in the data acquisition program.

ANTICIPATED RESULTS

This protocol, which is based on ref. 13, provides potential users a guideline on how to apply fPAM to noninvasive *in vivo* imaging. When operated correctly, fPAM is able to provide high-quality volumetric images of subcutaneous structures, which can be visualized by commercially available software packages (VolView, Kitware). Sample volumetric visualization results, in which the PA signals originating from the skin surface are removed, can be found in **Figure 2c** of this article and in Figure 2b of ref. 14.

Besides direct volumetric visualization, 2D images including B-scan images and maximum amplitude projection (MAP) images¹³ are adequate in many applications. A B-scan image of microvasculature can be found in **Figure 2b** and B-scan images of skin burns can be found in Figures 2c and 3a–d of ref. 17. Because fPAM uses an ultrasonic detector with large NA, the focal zone can be shorter than the desired FOV along the z axis, which results in degraded lateral resolution outside the ultrasonic focal zone. Hence for samples with large variations in skin contour, a post-processing method, referred to as the virtual-point-detector-based synthetic-aperture focusing technique²², can be used to improve the out-of-focus lateral resolution numerically. To obtain high-quality MAP images in fPAM, PA signals generated from the skin surface must be removed completely, which can be achieved manually. Users can first select several B-scan images from the acquired volume data and manually pick a few points on the skin surface in each B-scan image (**Fig. 2b**). Then, users can perform a 2D spline interpolation based on the recorded points on the skin surface and their horizontal coordinates to extract the skin profile for the whole volumetric image. Finally, users can set PA signals within a certain layer around the detected skin surface to zero so as to remove the skin signals. The thickness of such a layer depends on the sample. This manual operation may take ~10 min to complete. The assumption behind this operation is that the contour of the skin surface does not vary drastically and an automatic skin signal detection algorithm is applicable. Typical MAP images can be found in Figures 2b and 3a of ref. 13 and in Figure 2a of ref. 14. Besides MAP images from the whole volume, MAP images from a series of subvolumes can be computed to depict depth information as demonstrated in Figure 4d of ref. 13. Users are referred to refs. 23,24 for a more comprehensive explanation on MAP operation.

In functional imaging using fPAM, relative concentration distributions of pigments or contrast agents are calculated. Users need to normalize each measured PA signal by the corresponding laser energy (measured by the photodiode) before applying a least-squares fit¹⁹. In some cases, users also need to compensate for the wavelength-dependent optical attenuation caused by the skin or other tissues in order to achieve accurate inversion. In our previous work of imaging of sO₂ in subcutaneous microvasculature^{13,15}, we acquired the wavelength-dependent compensation coefficients by measuring PA signals generated from a subcutaneously inserted black target, which has spectrally uniform optical absorption within a wide spectral range (please refer to ref. 19 for more details). This invasive method provides a first-order estimation of the wavelength-dependent optical fluence attenuation in the skin. Sample MAP images of sO₂ in the subcutaneous microvasculature can be found in Figure 3b of ref. 13 and in Figure 2b of ref. 15, where venous and arterial blood vessels are separated based on the imaged sO₂. Images of variations in sO₂ in veins and arteries associated with systemic physiological modulations can be found in Figure 2c,d of ref. 15.

Noninvasive estimation of the wavelength-dependent optical fluence variation is also possible. One reported method²⁵ achieves this goal by solving the optical diffusion equation and the PA wave equation based on PA detection only. This method produces good results in tissue phantoms. As PA imaging filters out spatially homogeneous optical energy deposition (specific absorption), smooth structures such as capillary beds are invisible at the current spatial resolution. Therefore, additional optical measurement²⁶ is likely to be required to provide robust estimation of the optical fluence. However, this topic is beyond the scope of this article.

ACKNOWLEDGMENTS We thank G. Stoica, O. Craciun, J. Oh, G. Ku, M.-L. Li, X. Xie, G. Lungu, R. Zemp and M. Sivaramakrishnan for experimental assistance. This work was sponsored by grants from the National Institutes of Health (R01 EB000712 and R01 NS46214 to L.V.W.).

COMPETING INTERESTS STATEMENT The authors declare no competing financial interests.

Published online at <http://www.natureprotocols.com>

Reprints and permissions information is available online at <http://npg.nature.com/reprintsandpermissions>

1. Xu, M. & Wang, L.V. Photoacoustic imaging in biomedicine. *Rev. Sci. Instrum.* **77**, 041101 (2006).
2. Wang, X. *et al.* Noninvasive laser-induced photoacoustic tomography for structural and functional imaging of the brain *in vivo*. *Nat. Biotechnol.* **21**, 803–806 (2003).
3. Hoelen, C.G.A., de Mul, F.F.M., Pongers, R. & Dekker, A. Three-dimensional photoacoustic imaging of blood vessels in tissue. *Opt. Lett.* **23**, 648–650 (1998).
4. Oraevsky, A.A. & Karabutov, A.A. Photoacoustic Tomography. in *Biomedical Photonics Handbook*, Vol. PM125 (ed. Vo-Dinh, T.) (CRC Press, Boca Raton, Florida, 2003).
5. Kruger, R.A., Liu, P., Fang, Y.R. & Appledorn, C.R. Photoacoustic ultrasound (PAUS)—reconstruction tomography. *Med. Phys.* **22**, 1605–1609 (1995).
6. Bell, A.G. On the production and reproduction of sound by light. *Am. J. Sci.* **20**, 305–324 (1880).
7. Diebold, G.J., Khan, M.I. & Park, S.M. Photoacoustic “signature” of particulate matter: optical production of acoustic monopole radiation. *Science* **250**, 101–104 (1990).
8. Tam, A.C. Applications of photoacoustic sensing techniques. *Rev. Mod. Phys.* **58**, 381–431 (1986).
9. O’Leary, M.A., Boas, D.A., Chance, B. & Yodh, A.G. Experimental images of heterogeneous turbid media by frequency-domain diffuse-photon tomography. *Opt. Lett.* **20**, 426–428 (1995).
10. Boas, D.A. *et al.* Imaging the body with diffuse optical tomography. *IEEE Signal Processing Mag.* **18**, 57–75 (2001).
11. Duck, F.A. *Physical Properties of Tissue* (Academy Press, London, 1990).
12. Maslov, K., Stoica, G. & Wang, L.V. *In vivo* dark-field reflection-mode photoacoustic microscopy. *Opt. Lett.* **30**, 625–627 (2005).
13. Zhang, H.F., Maslov, K., Stoica, G. & Wang, L.V. Functional photoacoustic microscopy for high-resolution and noninvasive *in vivo* imaging. *Nat. Biotechnol.* **24**, 848–851 (2006).
14. Zhang, H.F., Maslov, K., Li, M.-L., Stoica, G. & Wang, L.V. *In vivo* volumetric imaging of subcutaneous microvasculature by photoacoustic microscopy. *Opt. Express.* **14**, 9317–9323 (2006).
15. Zhang, H.F., Maslov, K., Sivaramakrishnan, M., Stoica, G. & Wang, L.V. Imaging of hemoglobin oxygen saturation variations in single vessels *in vivo* using photoacoustic microscopy. *Appl. Phys. Lett.* **90**, 052901 (2007).
16. Oh, J.-T., Li, M.-L., Zhang, H.F., Maslov, K., Stoica, G. & Wang, L.V. Three-dimensional imaging of skin melanoma *in vivo* by dual-wavelength photoacoustic microscopy. *J. Biomed. Opt.* **11**, 034032 (2006).
17. Zhang, H.F., Maslov, K., Stoica, G. & Wang, L.V. Imaging acute thermal burns by photoacoustic microscopy. *J. Biomed. Opt.* **11**, 054033 (2006).
18. Li, L., Zemp, R.J., Lungu, G., Stoica, G. & Wang, L.V. Imaging of gene expression *in vivo* with photoacoustic tomography. *Proc. SPIE* **6086**, 62–67 (2006).
19. Maslov, K., Sivaramakrishnan, M., Zhang, H.F., Stoica, G. & Wang, L.V. Technical considerations in quantitative blood oxygenation measurement using photoacoustic microscopy *in vivo*. *Proc. SPIE* **6086**, 215–225 (2006).
20. Briggs, G.A.D. *Acoustic Microscopy* (Clarendon, Oxford, 1992).
21. Laser Institute of America, *American National Standard for Safe Use of Lasers ANSI Z136.1-2000*, (American National Standards Institute Inc., New York, NY, 2000).
22. Li, M.-L., Zhang, H.F., Maslov, K., Stoica, G. & Wang, L.V. Improved *in vivo* photoacoustic microscopy based on a virtual-detector concept. *Opt. Lett.* **31**, 474–476 (2006).
23. Brown, D.G. & Riederer, S.J. Contrast-to-noise ratio in maximum intensity projection images. *Magn. Reson. Med.* **23**, 130–137 (1992).
24. Anderson, C.M., Saloner, D., Tsuruda, J.S., Shapeero, L.G. & Lee, R.E. Artifacts in maximum-intensity-projection display of MR angiograms. *Am. J. Roentgenol.* **154**, 623–629 (1990).
25. Laufer, J., Deply, D., Elwell, C. & Beard, P. Quantitative spatially resolved measurement of tissue chromophore concentrations using photoacoustic spectroscopy: application to the measurement of blood oxygenation and haemoglobin concentration. *Phys. Med. Biol.* **52**, 141–168 (2007).
26. Wilson, B.C. & Jacques, S.L. Optical reflectance and transmittance of tissues: principles and applications. *IEEE J. Quant. Electron.* **26**, 2186–2199 (1990).

